

Research Article

Editable-DeepSC: Reliable Cross-Modal Semantic Communications for Facial Editing

Bin Chen¹, Wenbo Yu², Qinshan Zhang², Tianqu Zhuang², Hao Wu^{2,3}, Yong Jiang², and Shu-Tao Xia²

1. School of Computer Science and Technology, Harbin Institute of Technology, Shenzhen 518055, China

2. Tsinghua Shenzhen International Graduate School, Tsinghua University, Shenzhen 518055, China

3. Shenzhen ShenNong Information Technology Co., Ltd., Shenzhen 518000, China

Corresponding author: Hao Wu; Email: wu-h22@mails.tsinghua.edu.cn

Abstract— Interactive computer vision (CV) plays a crucial role in various real-world applications, whose performance is highly dependent on communication networks. Nonetheless, the data-oriented characteristics of conventional communications often do not align with the special needs of interactive CV tasks. To alleviate this issue, the recently emerged semantic communications only transmit task-related semantic information and exhibit a promising landscape to address this problem. However, the communication challenges associated with Semantic Facial Editing, one of the most important interactive CV applications on social media, still remain largely unexplored. In this paper, we fill this gap by proposing Editable-DeepSC, a novel cross-modal semantic communication approach for facial editing. Firstly, we theoretically discuss different transmission schemes that separately handle communications and editings, and emphasize the necessity of Joint Editing-Channel Coding (JECC) via iterative attributes matching, which integrates editings into the communication chain to preserve more semantic mutual information. To compactly represent the high-dimensional data, we leverage inversion methods via pre-trained StyleGAN priors for semantic coding. To tackle the dynamic channel noise conditions, we propose SNR-aware channel coding via model fine-tuning. Extensive experiments indicate that Editable-DeepSC can achieve superior editings while significantly saving the transmission bandwidth, even under high-resolution and out-of-distribution (OOD) settings.

Keywords— Semantic Communications, Cross-Modal Data, Facial Editing Tasks, Generative Adversarial Networks, Deep Learning.

I. Introduction

In the era of rapid technological advancement, interactive computer vision (CV) plays a pivotal role in various real-world applications, such as digital manufacturing [1], telemedicine [2], robotics [3], and metaverse [4]. The performance of interactive CV tasks is heavily dependent on the underlying communication networks. These traditional communication systems are primarily designed for data-oriented purpose and focus on metrics that measure the data transmission instead of tasks execution performance. In other words, the original data is expected to be completely recovered at the receiver side regardless of the users' usage about it. Nonetheless, this data-oriented design principle is not always suitable for the specific needs of interactive CV tasks, as different tasks at the receiver side would require different types of extracted semantic information from the original data, which should be encoded and transmitted with different importance. Reconstructing every part of the original data equally will undoubtedly waste the limited transmission bandwidth.

To alleviate this issue, the recently emerged semantic communications [5–10] (also known as task-oriented communications) only transmit the specific semantic information suitable for interactive CV tasks and exhibit a promising landscape to address this problem. By bridging the gap between bit-level transmission and task-oriented requirements, semantic communications can exploit much more of the scarce bandwidth to transmit task-related information, thus realizing better interactive CV tasks execution performance. On the other hand, Semantic Facial Editing [11–16], which stands out as one of the most important interactive CV tasks for user interaction and personalization, encounters various communication challenges when promoting its real-world deployment. As shown in Figure 1, in many famous social platforms (e.g., Facebook, Instagram), before transmitting their own photos to the remote servers, users may wish to flexibly edit the original data according to their personal needs, such as adding smile to a face or altering the transparency of eyeglasses. Furthermore, such personal requirements can be fulfilled by providing dialogues to enable a more conver-

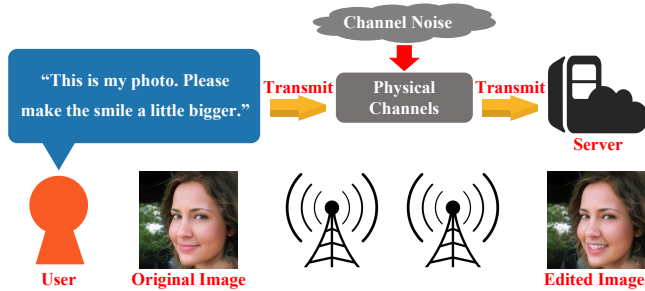


Figure 1 Illustration of the dynamic semantic facial editing scenarios. During the transmission, users may wish to flexibly edit the original multimedia data according to their personal needs in a conversational and interactive way.

sational and interactive experience. A crucial question still remains largely unexplored in existing works: *How to better transmit the facial semantics while also dynamically editing them according to the users' needs?*

In this paper, we fill this gap by proposing Editable-DeepSC, a novel cross-modal semantic communication approach for facial editing. Editable-DeepSC takes cross-modal text-image pairs as the inputs and transmits the edited semantic information of facial images based on textual instructions. For such dynamic facial editing and communication scenarios, Editable-DeepSC faces the following challenges:

- Q_1 : *How to better compress the original data, so that satisfying editing effects can be achieved with less transmission bandwidth consumption?*
- Q_2 : *How to better realize a trade-off between editing effects and fidelity, so that targeted semantics are edited while other untargeted semantics still remain unaffected?*
- Q_3 : *How to better tackle the dynamically varying channel conditions, so that the model can generalize well to different circumstances of communication capabilities?*

To address the above challenges, we propose Editable-DeepSC, a novel framework that integrates facial editing directly into the semantic communication chain. Unlike conventional separate schemes (where editing is performed either before or after transmission) that introduce redundant data processing procedures and risk losing semantic mutual information, our approach employs a joint optimization strategy to preserve semantic fidelity and enhance editing quality.

Editable-DeepSC operates through three cohesive stages. First, it leverages generative priors for efficient semantic coding, dramatically compressing high-dimensional facial images into low-dimensional representations to tackle Q_1 . Second, it introduces a Joint Editing-Channel Coding (JECC) mechanism that simultaneously performs semantic editing and ensures robustness against channel noise, addressing the fine-grained control requirements of Q_2 . Finally, an SNR-aware adaptation mechanism enables the model to efficiently

generalize across diverse channel conditions by fine-tuning only a minimal set of parameters, effectively solving Q_3 .

To verify the effectiveness of Editable-DeepSC, we conduct extensive experiments under various levels of SNRs and compare it with the baselines that separately handle communications and editings, where both editings after the channel transfer and before the channel transfer are evaluated. We also consider more rigorous and realistic simulation settings where the transmitter side users may hold high-resolution images or out-of-distribution (OOD) images. Numerous results indicate that Editable-DeepSC achieves superior editing effects compared to the baselines while significantly saving the transmission bandwidth. For instance, in high-resolution settings, Editable-DeepSC only consumes less than 2% of the baseline methods' bandwidth, but still achieves the best editing performance both quantitatively and qualitatively. Furthermore, in the fine-tuning stage, Editable-DeepSC only adjusts 2.65% of the total parameters, but still considerably improves the editing effects under low SNRs and protects the edited semantics from channel noise corruptions.

To the best of our knowledge, we are the first to systematically and comprehensively investigate the communication problems of dynamic facial editing in this research field. Our main contributions are as follows:

- We theoretically analyze different transmission schemes that separately handle communications and editings, encompassing both transmitter-side (pre-channel) and receiver-side (post-channel) editings. We discover that they actually increase the data processing procedures and are more likely to lose semantic mutual information, undermining efficiency and ultimately degrading received image quality. In light of this, we emphasize the necessity to integrate editings into the communication chain, jointly optimize these two aspects, and minimize the data processing procedures to preserve more semantic mutual information.
- We propose semantic coding via Generative Adversarial Networks (GAN) inversion. By leveraging the abundant generative priors within the pre-trained StyleGAN, we encode the high-dimensional input images into the GAN latent space and map them to low-dimensional representations. Thus, we compactly represent the high-dimensional input data and considerably decrease the Channel Bandwidth Ratio (CBR) required to transmit the edited facial semantics.
- We introduce Joint Editing-Channel Coding (JECC) via iterative attributes matching. By employing low-complexity Fully Connected Layers and an attribute-matching loop, we iteratively exert minor modifications on the results of semantic coding to realize semantic editing and channel coding at the same time. Thus, we reduce the data processing procedures for semantic mutual information preservation and precisely

perform fine-grained editings only on the targeted semantics, without influencing other untargeted ones.

- We present SNR-aware channel coding via model fine-tuning. We introduce two lightweight trainable adapters (which do not change the shapes of inputs and outputs within the JECC codecs) to capture the distribution of new noise conditions. When fine-tuning the models, only the parameters of these two adapters are adjusted to learn the characteristics of new transmission environments. Meanwhile, the rest of the parameters are frozen to avoid forgetting the previously learned priors due to the fine-tuning. This helps the model generalize well to the varying communication capabilities via minimal parameters fine-tuning.
- Extensive experiments demonstrate that Editable-DeepSC achieves superior performance compared to existing methods on editing effects and transmission efficiency, even under more practical settings with high-resolution and out-of-distribution (OOD) images.

The rest of this paper is organized as follows. Section 2 illustrates the related works. Section 3 introduces the system model. Section 4 elaborates on the implementation of Editable-DeepSC. Section 5 provides the experiment results. Section 6 concludes this work.

II. Related Work

1. Semantic Facial Editing

Semantic Facial Editing aims to provide personalized facial manipulations specified by the users, and has emerged as one of the most important interactive CV tasks for its wide range of applications, including virtual content creation [17], augmented reality (AR) [18], and online conferencing [19]. This technology enables users to make intuitive edits to facial attributes such as expression, age, hairstyle, offering both creative flexibility and enhanced user experiences.

In the early stage of this area, many methods [12, 13] focus on editing specific attributes, and rely heavily on extra manually provided knowledge such as landmarks. Recently, latent space based facial editing methods [14–16] are proposed due to the advancement of generative models like StyleGAN [20]. These methods typically strive to find semantically meaningful directions in the latent space of pre-trained generative models, so that shifting along the latent space would be able to achieve the desired editing in the vision space. InterFaceGAN [14] finds a hyperplane in the latent space to disentangle the facial semantics, and uses the normal vector of the hyperplane as the editing direction. Zhuang *et al.* [15] proposed to learn a mapping network to generate identity-specific directions within the latent space. However, both the two methods [14, 15] neglect language guidance and lack conversational interaction. To alleviate this issue, Jiang *et al.* [16] proposed Talk2Edit, which enables customized editings via human language feedback.

While diffusion models have recently gained significant popularity in image editing tasks [21], and have indeed been explored in semantic communications [22], we specifically choose the GAN architecture for Editable-DeepSC due to several practical advantages it offers. First, GAN-based models provide a well-structured latent space that enables more precise and disentangled control over facial attributes [20], which is crucial for achieving the fine-grained editing capabilities required by our framework. Second, the iterative denoising process of diffusion models typically requires multiple forward passes during inference [21], which would introduce substantial latency incompatible with interactive scenarios. In contrast, GAN models can be optimized to achieve a better balance between efficiency and quality, making it more suitable for our communication-efficient framework.

2. Task-Oriented Semantic Communications

Semantic communications prioritize the transmission of task-related semantic information rather than the original data with enhanced communication efficiency, and have showed great potential across various CV tasks.

Single-modal semantic communications for image tasks. Zhang *et al.* [5] proposed a DNN-based image semantic communication system, which only transmits the gradients back to the transmitter during training to protect the receiver's privacy of downstream tasks. Xie *et al.* [23] proposed an image semantic communication method with the joint control of shallow and deep networks. Han *et al.* [24] proposed Standards-Compatible Semantic Communication (SCSC), an end-to-end image transmission approach with learnable preprocessing-empowered and precoder/combiner-enhanced modules for MIMO channels.

Single-modal semantic communications for video tasks. Jiang *et al.* [6] proposed a video semantic coding network based on keypoints transmission, and considerably reduced resources consumption without losing the main details. Wang *et al.* [7] exploited nonlinear transform and conditional coding architecture to adaptively extract semantic features across video frames, and surpassed traditional wireless video coded transmission schemes. Li *et al.* [25] proposed a video semantic communication system based on major object extraction and contextual video encoding, which can achieve efficient video transmission for massive communication.

Semantic communications for multi-modal/cross-modal CV tasks. Xie *et al.* [8] proposed a multi-modal semantic communication system for Visual Question Answering (VQA) tasks, which utilizes MAC networks [26] to deal with the interconnected cross-modal data and generate the answers to VQA tasks. Jiang *et al.* [27] proposed a novel Vision-Language Model-based Cross-modal Semantic Communication (VLM-CSC) system, which consists of three innovative components: Cross-modal Knowledge Base (CKB), Memory-assisted Encoder and Decoder (MED), and Noise Attention Module (NAM). VLM-CSC effectively addresses

the challenges in dynamic environments such as low information density and catastrophic forgetting. Tian *et al.* [28] proposed a synchronous multi-modal semantic communication System with packet-level coding (SyncSC) for facial video and speech transmission, which reduces transmission overhead while ensuring high-quality synchronous transmission of video and speech over the packet loss network.

However, to the best of our knowledge, the cross-modal semantic communication challenges under dynamic facial editing scenarios have not yet been systematically explored up to now. In this paper, we aim to fill this gap and comprehensively address these problems.

III. System Model

As shown in Figure 2, our proposed Editable-DeepSC mainly consists of the Text Semantic Encoder, the Image Semantic Encoder, the Joint Editing-Channel Encoder, and the Joint Semantic-Channel Decoder, where channel noise corruptions from the real world are also taken into consideration. A summary of used mathematical symbols throughout this paper is shown in Table 1.

1. Semantic Transmitter

The input image $S_I \in \mathbb{R}^{1 \times C \times W \times H}$ (where H , W , and C represent the image's height, width, and color channels) is first transformed by the Image Semantic Encoder into low-dimensional representations for data compression, i.e.,

$$E_I = \mathcal{SE}_I(S_I; \alpha), \quad (1)$$

where $E_I \in \mathbb{R}^{1 \times L_1}$ (with L_1 being the dimension of visual features) is the extracted image semantic information and $\mathcal{SE}_I(\cdot; \alpha)$ denotes the Image Semantic Encoder with the parameters α . Similarly, the corresponding instructive sentence $S_T \in \mathbb{R}^{1 \times L_2 \times L_3}$ (where L_2 is the text length and L_3 is the dimension of textual embeddings) is also encoded by the Text Semantic Encoder $\mathcal{SE}_T(\cdot; \beta)$ with the parameters β to acquire the textual semantic information $E_T \in \mathbb{R}^{1 \times L_4}$ (with L_4 being the dimension of textual features), which is highly relevant to the anticipated editing:

$$E_T = \mathcal{SE}_T(S_T; \beta). \quad (2)$$

Next, E_I and E_T are sent into the Joint Editing-Channel Encoder $\mathcal{JEC}(\cdot, \cdot; \gamma)$ with the parameters γ , which will apply semantic editing as well as channel coding to the transmitted information in the meantime:

$$X = \mathcal{JEC}(E_I, E_T; \gamma). \quad (3)$$

The output of $\mathcal{JEC}(\cdot, \cdot; \gamma)$, i.e., $X \in \mathbb{C}^{1 \times k}$ (where k is the length of X), is then transmitted through the physical channels. We enforce an average transmission power constraint on X to ensure that it does not exceed the limits of current communication capabilities:

$$\frac{1}{k} \cdot \|X\|_2^2 \leq P_{max}, \quad (4)$$

where P_{max} is the power constraint.

Following the previous works [29–31] in this research field, the Channel Bandwidth Ratio (CBR) can be defined as:

$$\rho = \frac{k}{H \times W \times C}. \quad (5)$$

Smaller ρ indicates better compression. In our framework, the GAN inversion process (detailed in Section 4.1) plays a central role in achieving a low CBR. It compresses the high-dimensional input image $S_I \in \mathbb{R}^{1 \times C \times W \times H}$ into a low-dimensional latent representation $E_I \in \mathbb{R}^{1 \times L_1}$. This latent vector E_I is further processed by the JECC encoder to constitute the signal $X \in \mathbb{C}^{1 \times k}$ for transmission, whose length k is also very small due to the previous compression step of GAN inversion, consequently resulting in smaller ρ .

2. Semantic Receiver

The transmitted signals are usually corrupted by the channel noise. Consequently, only the disrupted forms of the edited semantic information can be detected at the receiver side, i.e.,

$$Y = h * X + N, \quad (6)$$

where $Y \in \mathbb{C}^{1 \times k}$ represents the received signal, $h \in \mathbb{C}$ denotes the channel coefficients, and $N \in \mathbb{C}^{1 \times k}$ denotes the Gaussian noise, whose elements (including the real and imaginary parts) are independent of each other and have the same mean and variance. Under simplified channel models such as the Additive White Gaussian Noise (AWGN) channel, h is typically a scalar constant (e.g., $h = 1$, representing no fading). In more general flat-fading channel models, h is a complex random variable following a certain distribution (e.g., Rayleigh, Rician) that characterizes the attenuation and phase shift introduced by the wireless channel. For simplicity, we consider $h = 1$ following the previous methods [9, 30].

Finally, Y is mapped back to the high-dimensional vision domain to get the edited image $\hat{S}_{I'} \in \mathbb{R}^{1 \times C \times W \times H}$ required by the transmitter:

$$\hat{S}_{I'} = \mathcal{JSCD}(Y; \theta), \quad (7)$$

where $\mathcal{JSCD}(\cdot; \theta)$ indicates the Joint Semantic-Channel Decoder with the parameters θ . It first acts as a channel decoder, where its internal components (e.g., lightweight adapters) work to correct the errors introduced by the noisy channel, effectively denoising the received signal Y . Subsequently, it functions as a semantic decoder and maps the partially corrected latent representations back to the high-dimensional image space, reconstructing the final edited image $\hat{S}_{I'}$. This integrated process ensures that semantic recovery and channel error correction are jointly optimized, rather than being treated separately, which will reduce the semantic errors caused by the channel noise. Moreover, since only the edited images are ultimately required and there is no need to reconstruct the instructive sentences, the Text Semantic Decoder is unnecessary in our model and thus not considered.

Table 1 Definitions of used symbols throughout this paper.

Symbol	Description	Symbol	Description
S_I	Input image, $\mathbb{R}^{1 \times C \times W \times H}$	S_T	Input sentence, $\mathbb{R}^{1 \times L_2 \times L_3}$
\hat{S}_I	Reconstructed (edited) image, $\mathbb{R}^{1 \times C \times W \times H}$	E_I	Image features, $\mathbb{R}^{1 \times L_1}$
E_T	Text features, $\mathbb{R}^{1 \times L_4}$	X	Transmitted signal, $\mathbb{C}^{1 \times k}$
Y	Received signal, $\mathbb{C}^{1 \times k}$	X', Y'	Signal after/before adapter, $\mathbb{C}^{1 \times k}$
h	Channel coefficient, \mathbb{C}	N	Gaussian noise, $\mathbb{C}^{1 \times k}$
$\mathcal{SE}_I(\cdot; \alpha)$	Image Semantic Encoder	$\mathcal{SE}_T(\cdot; \beta)$	Text Semantic Encoder
$\mathcal{JECCE}(\cdot, \cdot; \gamma)$	Joint Editing-Channel Encoder	$\mathcal{JSCD}(\cdot; \theta)$	Joint Semantic-Channel Decoder
$\mathcal{ACE}(\cdot; \phi)$	Channel Encoder Adapter	$\mathcal{ACD}(\cdot; \psi)$	Channel Decoder Adapter
$G(\cdot)$	Pre-trained StyleGAN Generator	$\mathcal{M}(\cdot; \gamma)$	Fully Connected Layers in $\mathcal{JECCE}(\cdot, \cdot; \gamma)$
$P(\cdot)$	Pre-trained attribute predictor	$D(\cdot)$	StyleGAN Discriminator
$F(\cdot)$	Pre-trained Face recognition model	z	Latent vector in StyleGAN space
$z^{(t)}$	Latent after t -th inversion iteration	$E_I^{(t)}$	Latent after t -th editing iteration
I_g	Image generated by $G(z)$	$J(z)$	Distortion in inversion
λ_{inv}	Weight for pixel-level distortion	η_{inv}	Learning rate for inversion
r_{inv}	Total inversion iterations	a_i	Degree of the i -th attribute
m	Total number of attributes	u	Maximum degree value for each attribute
i_{tar}	Index of targeted attribute	d_{tar}	Editing direction (-1 or $+1$)
Δ_{tar}	Degree of modification	a_{exp}	Expected attribute degree
r_{edit}	Maximum editing iterations	b_{ij}	One-hot of expected attribute degrees
p_{ij}	Predicted probability of attribute i degree j	\mathcal{L}_{pred}	Predictor loss
\mathcal{L}_{id}	Identity preservation loss	\mathcal{L}_{disc}	Discriminator loss
$\lambda_{pred}, \lambda_{id}, \lambda_{disc}$	Loss weights for training JECC codecs	I_a, I_b	Images after/before editing
n_{ft}	Number of fine-tuning images	\mathcal{L}_{ft}	Fine-tuning loss
η_{ft}	Fine-tuning learning rate	r_{ft}	Fine-tuning iterations
P_{max}	Average transmission power constraint	ρ	Channel Bandwidth Ratio (CBR)
K_0	Distribution of original images	K_n	Distribution of final edited images
K_s	Distribution of intermediate representations	$\mathcal{I}(\cdot; \cdot)$	Mutual information

3. Theoretical Rationality

To justify the rationality of our proposed Editable-DeepSC, we consider the alternative separate schemes below and theoretically demonstrate the superiority of our approach. Specifically, based on the sequence of communications and editings, we consider the following separate schemes:

M_1 : (editings after the channel transfer) The transmitter sends the images, and then the receiver edits them.

M_2 : (editings before the channel transfer) The transmitter edits the images, and then sends them to the receiver.

For the encoding and decoding steps of DNN as well as the channel transfer steps, the outputs of each stage are largely dependent on the current inputs instead of the previous outputs, which approximately satisfies the Markov property. Thus, as suggested in many previous works [32–34], we approximate the above encoding, decoding, and channel transfer steps as a Markov chain $K_0 \rightarrow K_1 \rightarrow \dots \rightarrow K_n$, where K_0 indicates the distribution of original images at the transmitter side, n is the total number of data processing procedures, K_n indicates the distribution of ultimate edited images at the receiver side, and K_s ($0 < s < n$) indicates the distribution of a series of intermediate representations during the above steps. For any two transitions $U \rightarrow V \rightarrow W$ from the whole Markov chain, we have the Data Processing Inequality (DPI) [35] as demonstrated in Theorem 1.

Theorem 1 (Data Processing Inequality) If $U \rightarrow V \rightarrow W$, then $\mathcal{I}(U; V) \geq \mathcal{I}(U; W)$.

By applying the DPI to the whole Markov chain $K_0 \rightarrow K_1 \rightarrow \dots \rightarrow K_n$ as pointed out in [32], we have $\mathcal{I}(K_0; K_1) \geq \mathcal{I}(K_0; K_2) \geq \dots \geq \mathcal{I}(K_0; K_n)$. This implies that as the data processing procedures increase, the semantic mutual information about the original distribution K_0 carried by the intermediate distribution K_s will decrease and cannot be recovered in the subsequent steps. Therefore, the aforementioned separate schemes M_1 and M_2 that have more encoding and decoding steps are more likely to lose semantic mutual information, which will eventually limit the quality of edited images. On the contrary, Editable-DeepSC integrates editings into the communication chain to decrease the data processing procedures, and will thus preserve more semantic mutual information with enhanced tasks performance.

IV. Method

This section elaborates the proposed Editable-DeepSC framework, whose overall pipeline and corresponding three-stage data flow are illustrated in Figure 3. The framework operates through three cohesive stages: (1) Semantic Coding via Pre-trained GAN Inversion; (2) Joint Editing-Channel Coding (JECC) via Iterative Attributes Matching; (3) SNR-aware Channel Coding via Model Fine-tuning.

In the first stage, the input facial image S_I and textual

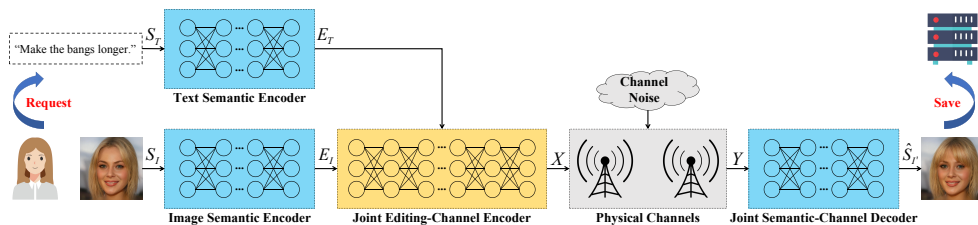


Figure 2 Overview of the proposed framework. Editable-DeepSC mainly consists of the Text Semantic Encoder, the Image Semantic Encoder, the Joint Editing-Channel Encoder, and the Joint Semantic-Channel Decoder, where channel noise corruptions from the real world are also considered.

instruction S_T are processed by the Image Semantic Encoder $\mathcal{SE}_I(\cdot; \alpha)$ and Text Semantic Encoder $\mathcal{SE}_T(\cdot; \beta)$, to extract compact latent representations E_I and E_T via GAN inversion. These representations then flow into the second stage, where the core JECC mechanism iteratively refines E_I guided by E_T to produce the transmitted signal X , simultaneously achieving semantic editing and channel coding. After transmission through a noisy channel $Y = h * X + N$, the third stage employs SNR-aware fine-tuning, where lightweight adapters within $\mathcal{JECCE}(\cdot, \cdot; \gamma)$ and $\mathcal{JSCD}(\cdot; \theta)$ are selectively updated to adapt to varying channel conditions, culminating in the generation of the final edited image \hat{S}_I by $\mathcal{JSCD}(\cdot; \theta)$. This integrated pipeline ensures precise execution of editings while maintaining robustness against channel noise, significantly reducing redundant data processing procedures compared to separate approaches.

1. Semantic Coding via Pre-trained GAN Inversion

We leverage the Generative Adversarial Networks (GAN) inversion methods [36–42] based on StyleGAN [20] priors to design the Image Semantic Encoder $\mathcal{SE}_I(\cdot; \alpha)$, as there is abundant prior knowledge within the pre-trained GAN to reduce the representation dimension. To be specific, given an input image S_I , a random vector z is first initialized in the StyleGAN latent space. The random vector z is then fed into the pre-trained StyleGAN Generator $G(\cdot)$ to generate an initial image $I_g = G(z)$. The distortion $J(z)$ between S_I and I_g is calculated as:

$$J(z) = \lambda_{inv} \cdot MSE(S_I, I_g) + LPIPS(S_I, I_g). \quad (8)$$

The distortion $J(z)$ is measured from both the pixel level and the perceptual level, balanced by the hyper-parameter λ_{inv} . In this paper, we adopt the MSE loss for the pixel level distortion and the LPIPS loss [43] for the perceptual level distortion. To obtain the latent vector that perfectly suits the original image, we can minimize $J(z)$ and update z by iteratively performing the gradient descent until convergence:

$$z^{(t)} = z^{(t-1)} - \eta_{inv} \cdot \nabla_{z^{(t-1)}} J(z^{(t-1)}), \quad (9)$$

where r_{inv} is the number of total inversion iterations, $z^{(0)}$ denotes the randomly initialized latent vector, $z^{(t)}$ ($1 \leq t \leq r_{inv}$) denotes the outcome after the t -th iteration, and η_{inv}

is the inversion learning rate. The learning rate η_{inv} is set to 0.10 to ensure stable convergence, and the maximum number of iterations r_{inv} is set to 110 based on a trade-off between reconstruction quality and computational cost, as analyzed in Section 5.5. The optimization process terminates when either the maximum iteration count r_{inv} is reached or the relative change in the distortion $J(z)$ between consecutive iterations falls below a threshold $\epsilon = 1 \times 10^{-5}$, i.e., $|J(z^{(t)}) - J(z^{(t-1)})| / |J(z^{(t-1)})| < \epsilon$. Upon completing the optimization of (9), we will obtain the output of semantic coding, which is denoted as $E_I = z^{(r_{inv})}$. Note that the dimension of z is often much smaller than the dimension of S_I , hence we can greatly compress the original data and reduce the Channel Bandwidth Ratio (CBR) defined in (5).

As for the Joint Semantic-Channel Decoder $\mathcal{JSCD}(\cdot; \theta)$, we first convert Y back to a real-valued latent representation, which is then sent to another pre-trained StyleGAN Generator for semantic decoding to map the compressed data back to high-dimensional images. Besides, we additionally introduce lightweight trainable parameters for channel decoding to reduce the semantic errors caused by the channel noise, which we will detailedly discuss in Section 4.3.

2. Joint Editing-Channel Coding (JECC) via Iterative Attributes Matching

Editing Attributes. Firstly, we need to quantitatively measure the attributes for editing (e.g., bangs, eyeglasses). We introduce an attribute predictor $P(\cdot)$ pre-trained on the CelebA-Dialog dataset [44], which consists of detailed manual annotations regarding the attributes of each training image. We send the original image to $P(\cdot)$ and obtain its output $\{a_1, a_2, \dots, a_i, \dots, a_m\}$, where the value of a_i indicates the degree of each attribute (e.g., the length of the bangs, the transparency of eyeglasses), m is the total number of attributes, and u is the same maximum degree value for each attribute.

Editing Semantic Information Extraction. We utilize the Long Short-Term Memory (LSTM) [45] network to implement the Text Semantic Encoder $\mathcal{SE}_T(\cdot; \beta)$, which can capture the dependencies between various parts of the input texts. We train $\mathcal{SE}_T(\cdot; \beta)$ on the CelebA-Dialog dataset [44] using the cross-entropy loss, where the training texts are manually annotated with their actual semantic information (i.e., the index of targeted attribute $i_{tar} \in \{1, 2, \dots, m\}$, the direc-

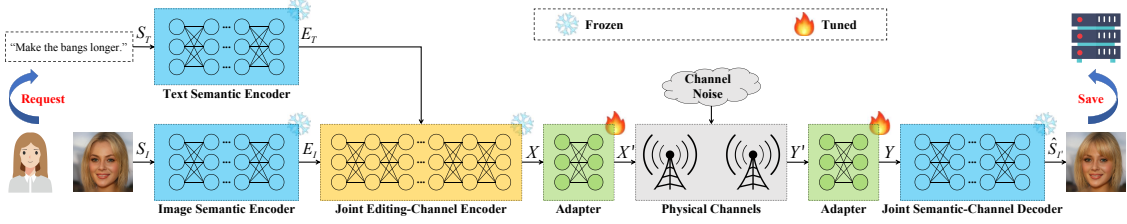


Figure 3 Illustration of our SNR-aware channel coding based on model fine-tuning. We introduce two lightweight trainable adapters that do not change the shapes of inputs and outputs to the Joint Editing-Channel Encoder and the Joint Semantic-Channel Decoder. When fine-tuning the models, only the parameters of these two adapters are adjusted to capture the distribution of new noise conditions, and the rest of the parameters are frozen to avoid forgetting the previously learned priors from Section 4.2.

tion of editing $d_{tar} \in \{-1, +1\}$, and the degree of modification $\Delta_{tar} \in \{0, 1, \dots, u\}$ as the labels. In the test time, the original texts are tokenized into words or subwords according to the dictionary and then sent to $\mathcal{SE}_{\mathcal{T}}(\cdot; \beta)$. The ultimate text encodings E_T will contain the aforementioned semantic information needed for editing: i_{tar} , d_{tar} and Δ_{tar} .

Joint Editing-Channel Coding (JECC). Inspired by the fact that DeepJSCC [46] combines source coding and channel coding to jointly optimize data compression and error correction, we implement the Joint Editing-Channel Encoder $\mathcal{JECC}(\cdot, \cdot; \gamma)$ by Fully Connected Layers $\mathcal{M}(\cdot; \gamma)$ to jointly optimize editings and communications for reduced data processing procedures. The Joint Editing-Channel Encoder $\mathcal{JECC}(\cdot, \cdot; \gamma)$ will iteratively exert minor modifications on the previous results of semantic coding to realize semantic editing and channel coding at the same time. Note that $\mathcal{M}(\cdot; \gamma)$ only takes E_I as the input, while E_T , the other input of $\mathcal{JECC}(\cdot, \cdot; \gamma)$, is utilized to obtain i_{tar} , d_{tar} and Δ_{tar} that guide the semantic editing. In the test time, we first compute the expected degree of targeted attribute by $\{a_1, a_2, \dots, a_i, \dots, a_m\}$, i_{tar} , d_{tar} , and Δ_{tar} :

$$a_{exp} = \min(\max(a_{i_{tar}} + \Delta_{tar} \cdot d_{tar}, 0), u), \quad (10)$$

where the minimum function $\min(\cdot, \cdot)$ and the maximum function $\max(\cdot, \cdot)$ are adopted to ensure that $0 \leq a_{exp} \leq u$. Then, we iteratively exert minor modifications on E_I :

$$E_{I'}^{(t)} = E_{I'}^{(t-1)} + d_{tar} \cdot \mathcal{M}(E_{I'}^{(t-1)}; \gamma), \quad (11)$$

where r_{edit} is the maximum number of total editing iterations, $E_{I'}^{(0)}$ is the same as E_I , and $E_{I'}^{(t)}$ ($1 \leq t \leq r_{edit}$) denotes the outcome after the t -th iteration. After each iteration of modification, $E_{I'}^{(t)}$ is delivered to the StyleGAN Generator $G(\cdot)$ to reconstruct an intermediate image, which will be sent to the pre-trained attribute predictor $P(\cdot)$ defined in [44] to check whether the anticipated requirement is satisfied. The predicted degree of the intermediate image calculated by $P(\cdot)$ will be compared with the expected degree a_{exp} . Once they match with each other, the iteration will stop and $E_{I'}^{(t)}$ will be used to form the complex-valued signal X (e.g., by treating

the first and second halves as the real and imaginary parts) for transmission. Otherwise, $\mathcal{M}(\cdot; \gamma)$ will continue to make small movements on $E_{I'}^{(t)}$ until the target is reached or the maximum number r_{edit} is exceeded.

Training Strategy of the JECC Codecs. To train $\mathcal{M}(\cdot; \gamma)$ for the i -th attribute, we set the expected degree of the i -th attribute to be $(a_i + 1)$ so that the model can learn how to perform fine-grained editings on each attribute. Note that the situation for $(a_i - 1)$ is completely symmetrical when d_{tar} is set to -1 . The predictor loss \mathcal{L}_{pred} can be calculated by adopting the cross-entropy loss:

$$\mathcal{L}_{pred} = - \sum_{i=1}^m \sum_{j=0}^u b_{ij} \cdot \log(p_{ij}), \quad (12)$$

where $b_{ij} \in \{0, 1\}$ is the one-hot representation of the expected attribute degrees, and p_{ij} is the output of the pre-trained attribute predictor $P(\cdot)$ on the edited image. We also leverage the identity preservation loss \mathcal{L}_{id} to better keep the original facial identity. We use ready-made facial recognition model to extract the features. The extracted features for facial recognition should be as similar as possible:

$$\mathcal{L}_{id} = \|F(I_a) - F(I_b)\|_1, \quad (13)$$

where I_a, I_b are the images after and before the editing, and $F(\cdot)$ is the pre-trained face recognition model [47]. The discriminator loss \mathcal{L}_{disc} is also adopted to ensure the fidelity on the generated images:

$$\mathcal{L}_{disc} = -D(I_a), \quad (14)$$

where $D(\cdot)$ is the output of the pre-trained StyleGAN [20] discriminator. Finally, the total loss can be calculated as:

$$\mathcal{L} = \lambda_{pred} \cdot \mathcal{L}_{pred} + \lambda_{id} \cdot \mathcal{L}_{id} + \lambda_{disc} \cdot \mathcal{L}_{disc}, \quad (15)$$

where λ_{pred} , λ_{id} , and λ_{disc} are the weight factors. We utilize the total loss \mathcal{L} to train $\mathcal{M}(\cdot; \gamma)$ through the noisy channels under high SNRs to guarantee their basic robustness against channel noises in addition to the semantic editing abilities. In our preliminary experiments, we find that if the training

SNRs are low, the editing effects are not satisfying because the extreme channel noises will instead disrupt the learning of semantic editing. Therefore, we train $\mathcal{M}(\cdot; \gamma)$ only under high SNRs and discuss how to fine-tune the JECC codecs under all levels of SNRs in Section 4.3.

3. SNR-aware Channel Coding via Model Fine-tuning

Benefiting from the recent successful applications of transfer learning techniques [48, 49], we propose SNR-aware channel coding based on model fine-tuning. As shown in Figure 3, we introduce two lightweight trainable adapters that consist of Fully Connected Layers and do not change the shapes of inputs and outputs to the Joint Editing-Channel Encoder $\mathcal{JECCE}(\cdot, \cdot; \gamma)$ and the Joint Semantic-Channel Decoder $\mathcal{JSCD}(\cdot; \theta)$. The complex-valued signal X is sent to the Channel Encoder Adapter $\mathcal{ACE}(\cdot; \phi)$ to obtain the final outcome of channel encoding:

$$X' = \mathcal{ACE}(X; \phi). \quad (16)$$

X' is then transmitted through the physical channels obeying the similar procedure described in (6) and the receiver will obtain Y' . Then, Y' is sent to the Channel Decoder Adapter $\mathcal{ACD}(\cdot; \psi)$ to acquire the new input of $\mathcal{JSCD}(\cdot; \theta)$:

$$Y = \mathcal{ACD}(Y'; \psi). \quad (17)$$

In the fine-tuning stage, we randomly select n_{ft} images that strictly have no intersections with the images used in the test time. For each new SNR level that needs to be adapted to, we transmit the fine-tuning images following the procedures defined in Section 3 as well as (16) and (17). We compute the LPIPS loss [43] between the final received image \hat{S}_I' and the original image S_I to measure the perceptual distortion for the fine-tuning loss \mathcal{L}_{ft} . We update the parameters of $\mathcal{ACE}(\cdot; \phi)$ and $\mathcal{ACD}(\cdot; \psi)$ using the gradient descent:

$$\begin{cases} \phi^{(t)} = \phi^{(t-1)} - \eta_{ft} \cdot \nabla_{\phi^{(t-1)}} \mathcal{L}_{ft} \\ \psi^{(t)} = \psi^{(t-1)} - \eta_{ft} \cdot \nabla_{\psi^{(t-1)}} \mathcal{L}_{ft}, \end{cases} \quad (18)$$

where r_{ft} is the number of total fine-tuning iterations, $\phi^{(t)}, \psi^{(t)}$ ($1 \leq t \leq r_{ft}$) are the results after the t -th iteration, and η_{ft} is the fine-tuning learning rate. When the fine-tuning is completed, these two adapters can capture the data distribution of current SNR level and enhance the perceptual quality of edited images in the test time, especially under extreme channel conditions. And the rest of the parameters are frozen to avoid forgetting the previously learned priors from Section 4.2 because of the fine-tuning. The algorithm framework of Editable-DeepSC is summarized in Algorithm 1.

V. Experiments

In this section, we conduct comprehensive experiments to evaluate the performance of the proposed Editable-DeepSC framework. First, the experimental setup (including datasets,

Algorithm 1 Editable-DeepSC Training Pipeline

Require: Training dataset \mathcal{D} ; Pre-trained models $G(\cdot), P(\cdot), F(\cdot)$; Hyper-parameters.

Ensure: Trained parameters $\gamma, \theta, \phi, \psi$.

- 1: **Stage 1: Semantic Coding via GAN Inversion**
- 2: **Goal:** Compress image S_I to latent code E_I .
- 3: Encode each $S_I \in \mathcal{D}$ by optimizing z to minimize distortion $J(z)$ between S_I and $G(z)$ as in (9).
- 4: Obtain semantic code $E_I = z^{(r_{inv})}$.
- 5: **Stage 2: JECC Training via Iterative Attributes Matching**
- 6: **Goal:** Learn joint editing-channel coding.
- 7: Encode text S_T to get editing targets $(i_{tar}, d_{tar}, \Delta_{tar})$ via $\mathcal{SE}_{\mathcal{T}}(\cdot; \beta)$.
- 8: Iteratively refine E_I using $\mathcal{M}(\cdot; \gamma)$ guided by editing targets as in (11).
- 9: Train γ, θ by minimizing $\mathcal{L} = \lambda_{pred} \mathcal{L}_{pred} + \lambda_{id} \mathcal{L}_{id} + \lambda_{disc} \mathcal{L}_{disc}$ under high SNRs.
- 10: **Stage 3: SNR-aware Model Fine-tuning**
- 11: **Goal:** Adapt to varying channel conditions.
- 12: For each target SNR, fine-tune adapters $\mathcal{ACE}(\cdot; \phi)$ and $\mathcal{ACD}(\cdot; \psi)$ as in (18).
- 13: Update ϕ, ψ by minimizing LPIPS loss \mathcal{L}_{ft} on a small image set. Freeze the other parameters.

baselines, and evaluation metrics) is introduced. The main results on the standard-resolution CelebA dataset [50] are then presented, followed by evaluations under more challenging high-resolution and out-of-distribution (OOD) scenarios. Finally, we provide detailed ablation studies and further analyses to verify the effectiveness of the key components and to gain deeper insights behind the method design.

1. Experiment Setup

Simulation Datasets. As for the textual instruction S_T , we use the editing requests from the CelebA-Dialog dataset [44] for all the experiments. As for the original image S_I : (1) In the main experiments, we consider relatively simple scenarios and choose from the CelebA dataset [50], whose images are cropped to the resolution of 128×128 and have similar distribution with the training set of StyleGAN [20]; (2) In the more realistic high-resolution experiments, we choose from the CelebA-HQ dataset [51] with the resolution of 1024×1024 ; (3) In the more realistic out-of-distribution (OOD) experiments, we choose from the MetFaces dataset [52] with the resolution of 128×128 , whose facial images are from artworks and have an inherent distribution bias with the natural facial images of StyleGAN training set. As for the fine-tuning images, we use images from the CelebA dataset [50] for the resolution of 128×128 , and use images from the CelebA-HQ dataset [51] for the resolution of 1024×1024 . We strictly ensure that the fine-tuning images are few in number ($n_{ft} < 20$) and have no intersections with the tested images.

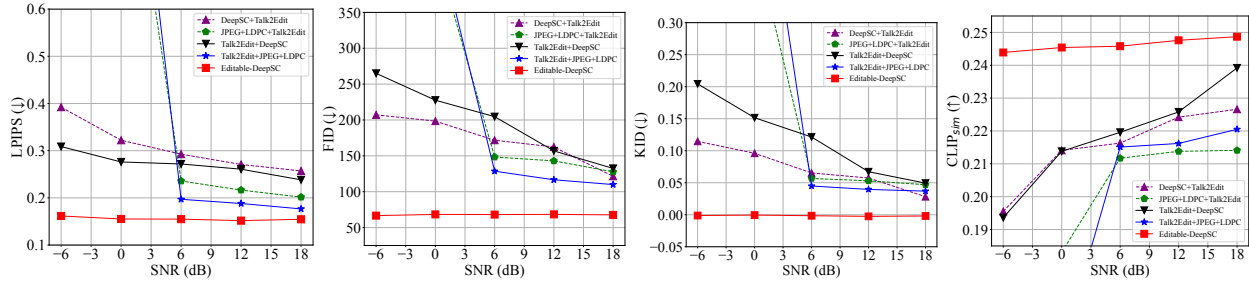


Figure 4 Quantitative comparison of different methods on the CelebA dataset (resolution 128×128) for cross-modal language-driven image editing and transmission tasks. Note that \downarrow indicates that the lower the metric, the better the performance, while \uparrow indicates that the higher the metric, the better the performance.

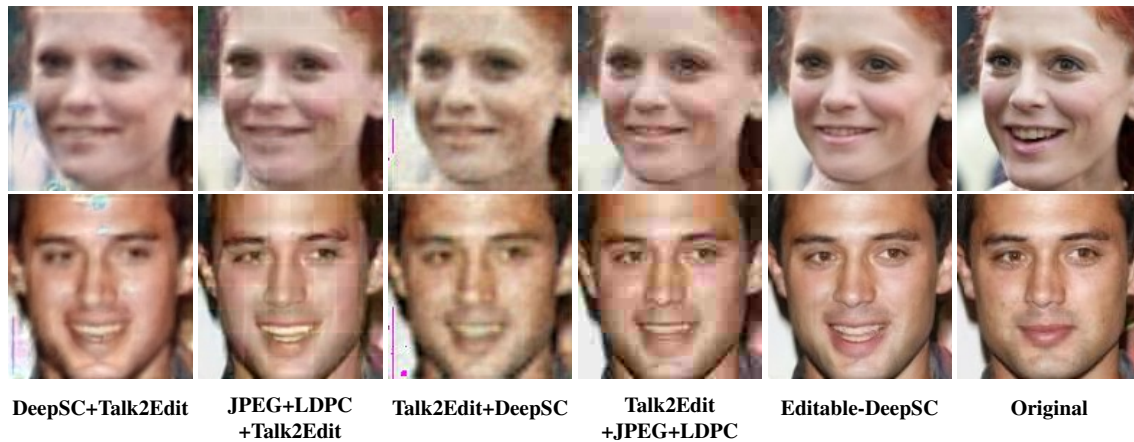


Figure 5 Qualitative comparison of different methods on the CelebA dataset (resolution 128×128) for cross-modal language-driven image editing and transmission tasks at the SNR of 6 dB. The instructive sentences for the 1st and 2nd rows are respectively “I kind of want the smile to be less obvious” and “Smile more”.

Evaluation Baselines. To the best of our knowledge, there exists no other semantic communication approach tailored for cross-modal facial editing tasks by now. Therefore, we compare Editable-DeepSC with the classical traditional communication methods JPEG [53] and LDPC [54], the novel single-modal image semantic communication method DeepSC [5], and the SOTA text-driven image editing method Talk2Edit [16] in the computer vision community. We rearrange these methods and consider the following baselines that separately handle communications and editings:

- **DeepSC+Talk2Edit.** DeepSC [5] is utilized to send S_I from the transmitter to the receiver. And the transmission of S_T is assumed to be error-free, which means that the received sentences are identical to the original ones to enhance the capabilities of this baseline for better persuasiveness. Then, Talk2Edit [16] is utilized to perform the text-driven image editing at the receiver side. This consists with the scheme M_1 mentioned in Section 3.3.
- **JPEG+LDPC+Talk2Edit.** JPEG [53] is utilized for image source coding and LDPC [54] is utilized for im-

age channel coding to send S_I from the transmitter to the receiver. And the transmission of S_T is also assumed to be error-free. Then, Talk2Edit [16] is utilized to perform the text-driven image editing at the receiver side. This consists with the scheme M_1 mentioned in Section 3.3.

- **Talk2Edit+DeepSC.** Talk2Edit [16] is utilized to perform the text-driven image editing at the transmitter side. Then, DeepSC [5] is utilized to send the edited images from the transmitter to the receiver. This consists with the scheme M_2 mentioned in Section 3.3.
- **Talk2Edit+JPEG+LDPC.** Talk2Edit [16] is utilized to perform the text-driven image editing at the transmitter side. Then, JPEG [53] is utilized for image source coding and LDPC [54] is utilized for image channel coding to send the edited images from the transmitter to the receiver. This consists with the scheme M_2 mentioned in Section 3.3.

Quantitative Metrics. To quantitatively measure the editing effects of different methods, we adopt LPIPS [43], FID [55], KID [56], and $CLIP_{sim}$ [57]. LPIPS utilizes pre-

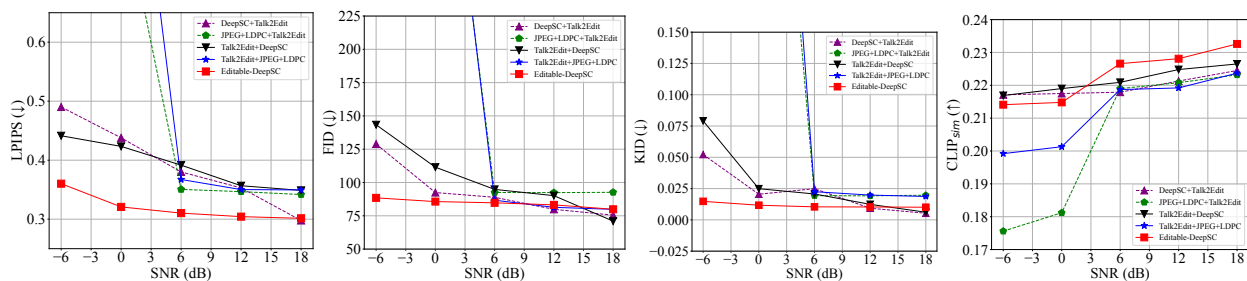


Figure 6 Quantitative comparison of different methods on the CelebA-HQ dataset (resolution 1024×1024) for cross-modal language-driven image editing and transmission tasks. Note that \downarrow indicates that the lower the metric, the better the performance, while \uparrow indicates that the higher the metric, the better the performance.

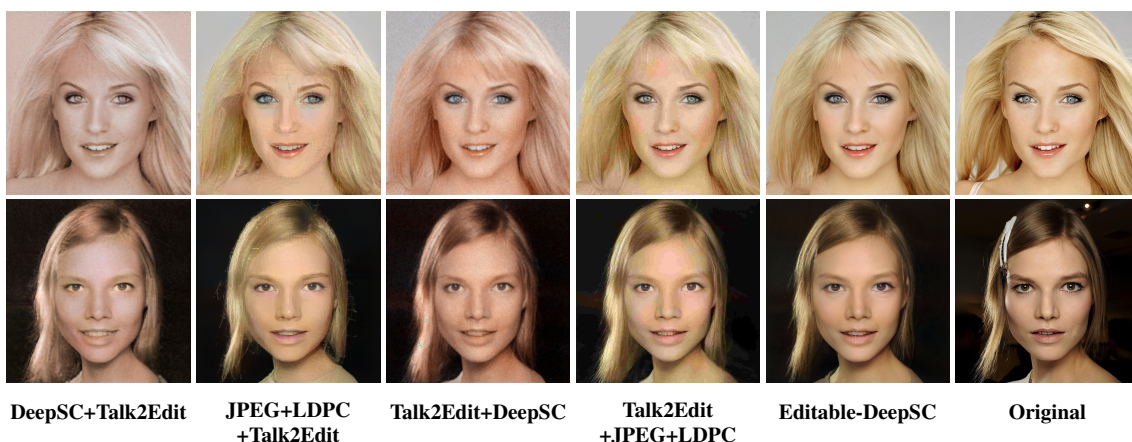


Figure 7 Qualitative comparison of different methods on the CelebA-HQ dataset (resolution 1024×1024) for cross-modal language-driven image editing and transmission tasks at the SNR of 6 dB. The instructive sentences for the 1st and 2nd rows are respectively “What about trying bangs that leaves half of the forehead visible” and “Make the face slightly younger”.

trained convolutional networks to extract the features of original images and edited images to calculate the perceptual differences. FID and KID computes the distribution differences between the original images and edited images. $CLIP_{sim}$ first utilizes the pre-trained CLIP models [57] to extract both the image and text features, and then computes the cosine similarity between the image features of edited results and the text features of target prompts to evaluate the semantic alignment with the editing instructions. Smaller LPIPS, FID, and KID scores indicate better visual fidelity, while higher $CLIP_{sim}$ scores indicate better editing effects. To quantitatively measure the communication efficiency, we adopt the Channel Bandwidth Ratio (CBR) defined in (5). Smaller CBR indicates better compression and communication efficiency.

Implementation Details. To simulate the varying communication circumstances, we set the SNR levels of -6 dB, 0 dB, 6 dB, 12 dB, 18 dB for all the methods. For Editable-DeepSC, λ_{inv} , η_{inv} , r_{inv} , η_{ft} , r_{ft} , and n_{ft} are set as 1.0 , 0.10 , 110 , 1×10^{-4} , 6 , and 10 , respectively. For DeepSC [5], the learning rate is set as 1×10^{-3} and the batch size is set as 4 . For JPEG [53] and LDPC [54], the target bpp under the resolution of 128×128 is set as 0.7 , the target bpp

under the resolution of 1024×1024 is set as 0.2 , and the Quadrature Amplitude Modulation (QAM) order is set as 4 . For Talk2Edit [16], we adopt its official code implementation. To ensure a fair comparison, the learning-based transmission approach, DeepSC [5], is first fully trained under each considered SNR level before testing. All the experiments are conducted on NVIDIA RTX A6000 GPUs.

2. Main Results

We compare Editable-DeepSC with the baselines on the CelebA dataset. From Figure 4, we find that Editable-DeepSC realizes the best results in terms of LPIPS, FID, KID, and $CLIP_{sim}$ with significant gains. For instance, when the SNR level is -6 dB, the LPIPS, FID, KID, and $CLIP_{sim}$ scores of Editable-DeepSC are improved by 47.65% , 67.82% , 101.05% , and 24.76% than the second best method, respectively. These results indicate that Editable-DeepSC achieves excellent editing effects with high fidelity and quality, outperforming the baselines that separately handle communications and editings. We also observe that the performance of JPEG+LDPC+Talk2Edit and Talk2Edit+JPEG+LDPC will decrease rapidly when the SNR level is below 6 dB, which is

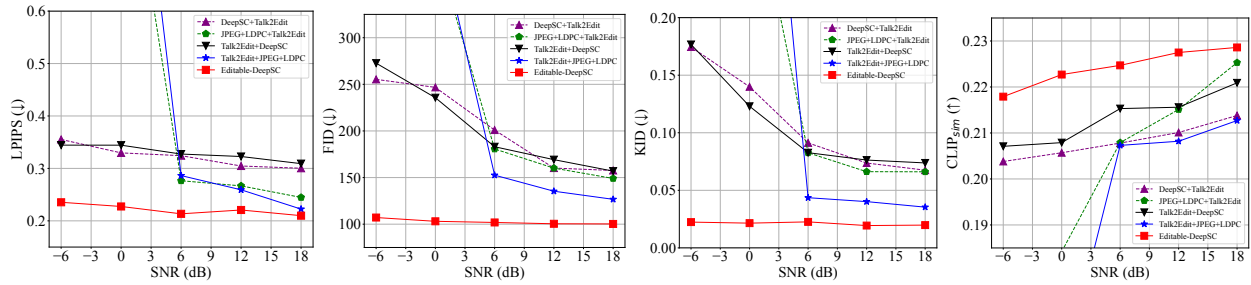


Figure 8 Quantitative comparison of different methods on the MetFaces dataset (resolution 128×128) for cross-modal language-driven image editing and transmission tasks. Note that \downarrow indicates that the lower the metric, the better the performance, while \uparrow indicates that the higher the metric, the better the performance.

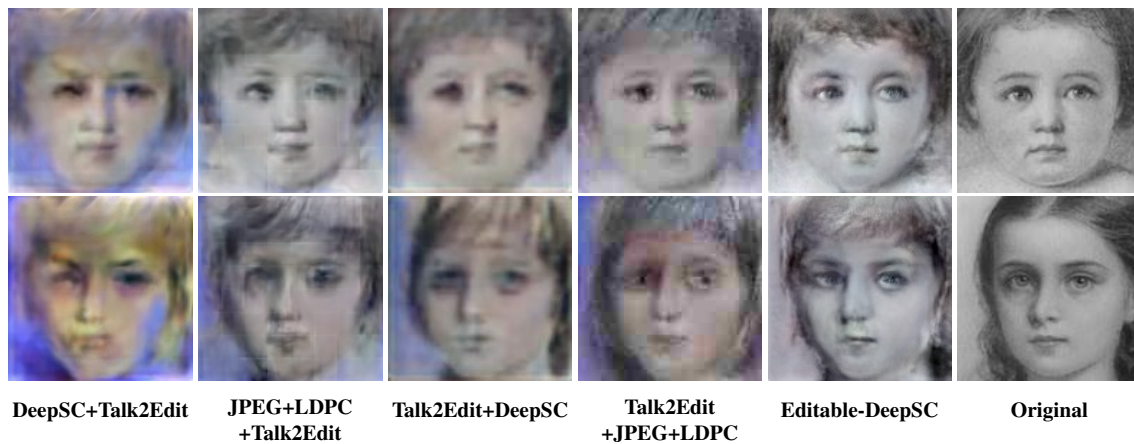


Figure 9 Qualitative comparison of different methods on the MetFaces dataset (resolution 128×128) for cross-modal language-driven image editing and transmission tasks at the SNR of 18 dB. The instructive sentences for the 1st and 2nd rows are respectively “Make the bangs longer” and “What about trying extremely long fringe”.

Table 2 Compression effectiveness of different methods with the resolution of 128×128 , measured by the Channel Bandwidth Ratio (CBR) defined in (5).

Method	Resolution	CBR (\downarrow)
DeepSC+Talk2Edit	128×128	0.0833
JPEG+LDPC+Talk2Edit	128×128	0.0389
Talk2Edit+DeepSC	128×128	0.0833
Talk2Edit+JPEG+LDPC	128×128	0.0389
Editable-DeepSC	128×128	0.0104

consistent with the fact that the traditional communications suffer greatly from the *cliff effect* [46].

Figure 5 illustrates the qualitative comparison of different methods at the noise level of 6 dB. We notice that Editable-DeepSC indeed achieves the best visualization results. Although the other methods also manage to edit the images, their effects are not as vivid and natural as those achieved with Editable-DeepSC. This is because Editable-DeepSC reduces the data processing procedures and preserves more semantic mutual information, which eventually leads to more satisfying editing results. Table 2 shows the compression ef-

fectiveness of different methods in terms of CBR defined in (5). We find that Editable-DeepSC only utilizes around 12.5% or 26.7% of the baselines' CBR, yet it still achieves extraordinary editing effects and outperforms all the baselines. Editable-DeepSC not only performs high-quality editings, but also considerably saves the transmission bandwidth.

3. High-Resolution Scenario Results

We then consider more realistic settings where the image resolution is expanded to 1024×1024 on the CelebA-HQ dataset. Figure 6 presents the LPIPS, FID, KID, and $CLIP_{sim}$ results while Table 3 presents the CBR results. The amplification of image pixels objectively increases the complexity of editing and transmission tasks. However, we find that Editable-DeepSC again achieves the best LPIPS scores under almost all the tested cases. As for the FID, KID, and $CLIP_{sim}$ scores, although Editable-DeepSC can't obtain the best results in some cases, it only uses around 0.2% or 1.8% of the baselines' CBR with much lower bandwidth costs as shown in Table 3. In general, Editable-DeepSC still exhibits great robustness and efficiency under high-resolution scenarios.

Figure 7 shows the visualization results of different meth-

Table 3 Compression effectiveness of different methods with the resolution of 1024×1024 , measured by the Channel Bandwidth Ratio (CBR) defined in (5).

Method	Resolution	CBR (\downarrow)
DeepSC+Talk2Edit	1024×1024	0.0833
JPEG+LDPC+Talk2Edit	1024×1024	0.0111
Talk2Edit+DeepSC	1024×1024	0.0833
Talk2Edit+JPEG+LDPC	1024×1024	0.0111
Editable-DeepSC	1024×1024	0.0002

ods on the CelebA-HQ dataset at the SNR of 6 dB. We notice that Editable-DeepSC can acquire better editing effects than the other methods, with fewer artifacts or blurs. In particular, for the 2nd row of images where the textual instruction is to make the face slightly younger, Editable-DeepSC manages to deal with this request in a fine-grained way and moderately alter the degree of youth. However, all the other methods overly modify the original face to appear too immature and there is the problem of excessive editing. This again validates the necessity to integrate editings into the communication chain for reduced data processing procedures, which can retain more semantic mutual information from the original images and precisely conduct fine-grained editings.

4. Out-Of-Distribution (OOD) Scenario Results

We also evaluate different methods under out-of-distribution (OOD) settings on the MetFaces dataset, where the distributions of training data and testing data are mismatched. From Figure 8, we observe that Editable-DeepSC continuously obtains the best LPIPS, FID, KID, and CLIP_{sim} scores. These results demonstrate that Editable-DeepSC possesses outstanding OOD generalizability, and is able to consistently surpass those baselines that separately communicate and edit even on unseen artistic datasets.

The visualization results in Figure 9 further demonstrate that Editable-DeepSC can precisely edit the OOD images without influencing other unrelated regions. In contrast, all the other methods struggle to realize the semantic editing while maintaining the fidelity, and encounter image quality degradation or even collapse under the more rigorous OOD scenarios. Our combination of editings and communications has indeed come into effect for better tasks performance.

5. Further Analysis

The influences of pre-trained GAN inversion. First, we explore the impacts of the proposed GAN inversion based semantic coding by changing the value of r_{inv} . From Table 4, we notice that when r_{inv} is small, increasing its value indeed improves the editing performance as the GAN inversion is more fully optimized, which validates the contribution of this component. However, when r_{inv} is large, further increasing its value cannot improve the editing performance and will also introduce more GPU energy costs. Thus, our adoption of $r_{inv} = 110$ is reasonable, for it strikes a better balance

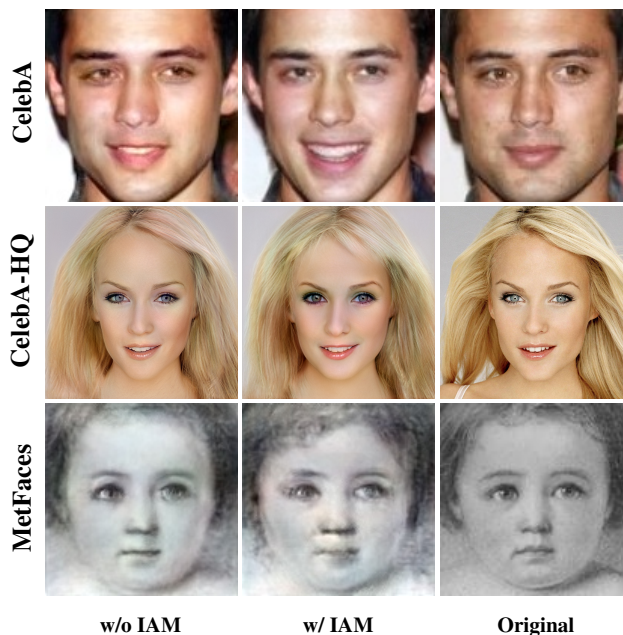


Figure 10 Qualitative results about whether the iterative attributes matching (IAM) mechanism is incorporated at the SNR of -6 dB. The instructive sentences for the 1st, 2nd, and 3rd rows are “Smile more”, “What about trying bangs that leaves half of the forehead visible”, and “Make the bangs longer”.

between editing effects and GPU energy costs.

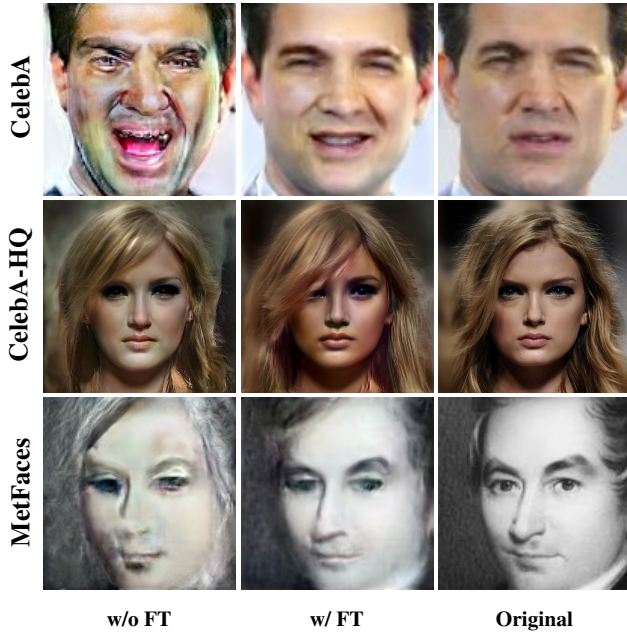
The influences of iterative attributes matching (IAM). Next, we study the impacts of the iterative attributes matching mechanism by removing it from Editable-DeepSC. As shown in Figure 10, when the iterative attributes matching mechanism is excluded, Editable-DeepSC will be unable to precisely perform the anticipated editings according to the given texts in a fine-grained way. This again provides evidence for the contribution of our IAM mechanism.

The influences of model fine-tuning. Similarly, we also investigate the impacts of the model fine-tuning mechanism in Table 4, Table 5, and Figure 11. We discover that under the extreme channel condition of -6 dB SNR, the fine-tuning mechanism plays a crucial role in preserving the quality and fidelity of edited images, while removing it will conversely generate unnatural or even collapsed regions. These results also verify the contribution of our fine-tuning mechanism. Moreover, our adoption of $r_{ft} = 6$ yields a satisfactory trade-off between fine-tuning effects and GPU energy costs.

Computational costs. Next, we provide analysis on computational costs. From Table 6, Editable-DeepSC has the smallest GPU energy costs and surpasses all the baselines. This is because Editable-DeepSC jointly optimizes the communications and editings with reduced data processing procedures, while the separate baselines repeatedly encode the data and result in low efficiency. Furthermore, Editable-DeepSC consumes less than 1600 MiB GPU memory for the reso-

Table 4 Quantitative results under different values of r_{inv} and r_{ft} on the CelebA dataset (resolution 128×128) at the SNR of -6 dB.

Metric	r_{inv}					r_{ft}				
	70	90	110	130	150	2	4	6	8	10
LPIPS (\downarrow)	0.1769	0.1633	0.1616	0.1642	0.1624	0.2110	0.1705	0.1616	0.1643	0.1645
FID (\downarrow)	67.02	66.99	66.64	68.75	71.12	84.24	71.39	66.64	69.21	70.63
KID (\downarrow)	0.0018	0.0009	-0.0012	-0.0005	-0.0010	0.0132	0.0004	-0.0012	-0.0007	-0.0003
CLIP _{sim} (\uparrow)	0.2296	0.2321	0.2439	0.2367	0.2358	0.2266	0.2364	0.2439	0.2310	0.2336
GPU Energy Costs (\downarrow)	252.19 mWh	308.19 mWh	362.05 mWh	419.49 mWh	470.95 mWh	358.26 mWh	360.74 mWh	362.05 mWh	363.61 mWh	367.26 mWh

**Figure 11** Qualitative results about whether the fine-tuning (FT) mechanism is incorporated at the SNR of -6 dB. The instructive sentences for the 1st, 2nd, and 3rd rows are “Smile more”, “Add long bangs”, and “Make the fringe just a little longer”.

lution of 128×128 and less than 3000 MiB GPU memory for the resolution of 1024×1024 . Thus, Editable-DeepSC achieves a good trade-off between utility and efficiency.

Parameters analysis. From Table 7, we note that the fine-tuned parameters only take up 2.65% of the total, while the remaining 97.35% of the total parameters are kept frozen. Nonetheless, the fine-tuning mechanism still results in significant performance gains. This further confirms the practicality and effectiveness of our fine-tuning method.

Ablation study on the channel decoder (CD) mechanism. In Table 8, we compare three variants: the full Editable-DeepSC model, a version where the channel decoder is pre-trained at a high SNR but tested at -6 dB (i.e., w/ weak CD), and a version where the channel decoder is completely removed (i.e., w/o CD). The results show that removing the channel decoder leads to the worst performance across all metrics, as the model performs semantic decoding directly on the severely corrupted received signal Y without any error correction. The weak CD variant shows intermediate performance, indicating that a channel decoder trained under a

Table 5 Quantitative results about whether the fine-tuning (FT) mechanism is incorporated at the SNR of -6 dB.

Dataset	Method	LPIPS (\downarrow)	FID (\downarrow)	KID (\downarrow)	CLIP _{sim} (\uparrow)
CelebA	w/o FT	0.3105	96.73	0.0292	0.2213
	w/ FT	0.1616	66.64	-0.0012	0.2439
CelebA-HQ	w/o FT	0.4790	100.03	0.0209	0.2022
	w/ FT	0.3602	88.47	0.0148	0.2141
MetFaces	w/o FT	0.3501	141.63	0.0821	0.2023
	w/ FT	0.2354	107.12	0.0224	0.2179

Table 6 GPU energy costs (\downarrow) of different methods averaged over each image under different resolutions.

Method	128×128	1024×1024
DeepSC+Talk2Edit	1432.94 mWh	3547.15 mWh
JPEG+LDPC+Talk2Edit	1540.53 mWh	3732.17 mWh
Talk2Edit+DeepSC	1462.73 mWh	3722.05 mWh
Talk2Edit+JPEG+LDPC	1485.72 mWh	3925.87 mWh
Editable-DeepSC	354.24 mWh	942.44 mWh

mismatched SNR condition still provides partial robustness, but is still significantly less effective than the properly fine-tuned decoder in the full model. These findings demonstrate the critical role of the SNR-aware channel decoder in mitigating semantic errors induced by channel noise.

Quantitative computation of mutual information (MI). In Section 3.3, we emphasize that the separate schemes introduce more data processing steps, which leads to the loss of semantic mutual information. To quantitatively validate this theoretical analysis, we employ the Mutual Information Neural Estimation (MINE) method [58] to estimate the MI between the original image distribution K_0 and the intermediate distribution K_s at different processing stages. The results are summarized in Table 9. We find that the MI values exhibit a monotonic decrease along the processing chain: $\mathcal{I}(K_0; K_1) > \mathcal{I}(K_0; K_2) > \mathcal{I}(K_0; K_3) > \mathcal{I}(K_0; K_4)$. This trend aligns well with the Data Processing Inequality (DPI). By integrating editing into the communication chain and reducing the number of separate steps, our proposed JECC framework effectively preserves more semantic mutual information about the original task, which is the fundamental reason for its superior performance over the separate baselines.

Component contribution analysis under varying channel conditions. Table 10 quantitatively analyzes the contribution of each key component under varying channel conditions. The full Editable-DeepSC model consistently achieves the highest CLIP_{sim} across all SNR levels, demonstrating the synergistic effect of its integrated design. The variant with

Table 7 The numbers of parameters in various parts of Editable-DeepSC. We also report the ratio of tuned parameters.

Frozen Parameters	Tuned Parameters	Total Parameters	Tuned Ratio
7.70×10^7	0.21×10^7	7.91×10^7	2.65%

Table 8 Quantitative results when adopting different variants of the channel decoder (CD) on the CelebA dataset at the SNR of -6 dB.

Model Variant	LPIPS (\downarrow)	FID (\downarrow)	KID (\downarrow)	CLIP (\uparrow)
Editable-DeepSC	0.1616	66.64	-0.0012	0.2439
w/ weak CD	0.2488	91.54	0.0102	0.2315
w/o CD	0.2965	103.81	0.0330	0.2305

weakened GAN inversion (adopting $r_{inv} = 70$) shows a consistent performance drop, indicating that high-fidelity semantic compression is foundational for preserving editing semantics. The most significant performance degradation, especially at medium-to-high SNRs, occurs when removing the Iterative Attributes Matching (IAM) mechanism, highlighting its critical role in achieving precise semantic alignment with text instructions. Conversely, the variant without fine-tuning (FT) suffers the most severe performance loss at low SNRs (e.g., -6 dB), underscoring that the SNR-aware adaptation module is primarily responsible for maintaining robustness in harsh channel conditions. In summary, GAN inversion provides the essential compressed representation, the JECC mechanism enables accurate editing, and fine-tuning ensures channel resilience. Their combination in Editable-DeepSC optimally balances these requirements for reliable cross-modal semantic communications.

Inference speed analysis. From Table 11, we find that the complete Editable-DeepSC framework is significantly faster than all separate baselines. The time of Editable-DeepSC is primarily consumed by the GAN inversion stage (7.79 seconds), which is an optimization-based process to find the optimal latent representation. The JECC iterative editing stage is highly efficient (only 0.35 seconds on average). While the current implementation does not achieve millisecond-level latency for strict real-time video streaming, the total processing time of around 10 seconds is highly suitable for interactive applications such as social media photo editing or cloud-based portrait enhancement, where users expect to wait several seconds for high-quality, personalized results. This demonstrates a favorable trade-off between the exceptional bandwidth efficiency (as shown in Table 2 and Table 3) and the achievable processing speed for interactive scenarios.

VI. Conclusion

In this paper, we propose Editable-DeepSC, a novel cross-modal semantic communication approach that tackles the communication challenges under dynamic facial editing scenarios. Specifically, we first theoretically analyze different transmission schemes that separately handle communications and editings. We find that they actually increase the data processing procedures and are more likely to lose semantic

Table 9 Estimated mutual information (MI) between the original distribution K_0 and the intermediate distributions at different processing stages. The decreasing MI along the processing chain aligns well with the Data Processing Inequality (DPI).

Distribution Pair	K_0, K_1	K_0, K_2	K_0, K_3	K_0, K_4	...
Mutual Information	2.6972	2.4683	1.8304	1.6627	...

Table 10 Component contribution analysis under varying channel conditions. We report the $CLIP_{sim}$ (\uparrow) values of different model variants on the CelebA dataset.

Model Variant	-6 dB	0 dB	6 dB	12 dB	18 dB
Editable-DeepSC	0.2439	0.2454	0.2458	0.2476	0.2487
w/ weak GAN inversion	0.2296	0.2329	0.2357	0.2371	0.2388
w/o IAM	0.2266	0.2304	0.2312	0.2297	0.2310
w/o FT	0.2213	0.2242	0.2318	0.2362	0.2366

mutual information. In light of this, we emphasize the necessity to integrate editings into the communication chain, jointly optimize these two aspects, and preserve more semantic mutual information. To compress the high-dimensional data, we leverage inversion methods based on pre-trained StyleGAN priors for semantic coding. To tackle the dynamic channel noise conditions, we propose SNR-aware channel coding based on model fine-tuning, which introduces two lightweight trainable adapters to capture the distribution of new noise conditions. Extensive experiments demonstrate that compared to existing methods, Editable-DeepSC exhibits superior editing effects while significantly saving the bandwidth under multiple settings.

Limitations and Feature Work. While Editable-DeepSC demonstrates significant advantages in various settings, we acknowledge the practical deployment challenges for resource-constrained mobile transmitters. The iterative closed-loop checks (e.g., StyleGAN generation and attribute prediction) indeed impose computational burdens. For future work, we hope to explore deployment strategies such as model distillation for lightweight edge deployment [59] or edge-cloud collaborative computing [60], enhancing practicality while preserving semantic communication benefits.

Acknowledgements

This work is supported in part by the National Natural Science Foundation of China under grant 62571298, 62576122,

Table 11 Inference speed comparison on the CelebA dataset. The time costs of GAN inversion and JECC iterations are also provided.

Method	Average Time (s)
DeepSC+Talk2Edit	35.16
JPEG+LDPC+Talk2Edit	36.36
Talk2Edit+DeepSC	35.26
Talk2Edit+JPEG+LDPC	35.68
GAN Inversion (Ours)	7.79
JECC Iterations (Ours)	0.35
Editable-DeepSC	10.78

62301189, and Shenzhen Science and Technology Program under Grant KJZD20240903103702004.

References

- [1] G. Chryssolouris, D. Mavrikios, N. Papakostas, D. Mourtzis, *et al.*, “Digital manufacturing: History, perspectives, and outlook”, *Proceedings of the Institution of Mechanical Engineers, Part B: Journal of Engineering Manufacture*, vol.223, no.5, pp.451–462, 2009.
- [2] C. O. Alenoghena, H. O. Ohize, A. O. Adejo, A. J. Onumanyi, *et al.*, “Telemedicine: A survey of telecommunication technologies, developments, and challenges”, *Journal of Sensor and Actuator Networks*, vol.12, no.2, article no.20, 2023.
- [3] M. Soori, B. Arezoo, and R. Dastres, “Artificial intelligence, machine learning and deep learning in advanced robotics, a review”, *Cognitive Robotics*, vol.3, pp.54–70, 2023.
- [4] H. Wang, H. Ning, Y. Lin, W. Wang, *et al.*, “A survey on the metaverse: The state-of-the-art, technologies, applications, and challenges”, *IEEE Internet of Things Journal*, vol.10, no.16, pp.14671–14688, 2023.
- [5] H. Zhang, S. Shao, M. Tao, X. Bi, and K. B. Letaief, “Deep learning-enabled semantic communication systems with task-unaware transmitter and dynamic data”, *IEEE Journal on Selected Areas in Communications*, vol.41, no.1, pp.170–185, 2023.
- [6] P. Jiang, C.-K. Wen, S. Jin, and G. Y. Li, “Wireless semantic communications for video conferencing”, *IEEE Journal on Selected Areas in Communications*, vol.41, no.1, pp.230–244, 2023.
- [7] S. Wang, J. Dai, Z. Liang, K. Niu, *et al.*, “Wireless deep video semantic transmission”, *IEEE Journal on Selected Areas in Communications*, vol.41, no.1, pp.214–229, 2023.
- [8] H. Xie, Z. Qin, and G. Y. Li, “Task-oriented multi-user semantic communications for vqa”, *IEEE Wireless Communications Letters*, vol.11, no.3, pp.553–557, 2022.
- [9] P. Wang, J. Li, M. Ma, and X. Fan, “Distributed audio-visual parsing based on multimodal transformer and deep joint source channel coding”, in *ICASSP 2022 - 2022 IEEE International Conference on Acoustics, Speech and Signal Processing (ICASSP)*, pp.4623–4627, 2022.
- [10] W. Yu, B. Chen, Q. Zhang, and S.-T. Xia, “Editable-deepscc: Cross-modal editable semantic communication systems”, in *2024 IEEE 99th Vehicular Technology Conference (VTC2024-Spring)*, pp.1–5, 2024.
- [11] H. Yang, D. Huang, Y. Wang, and A. K. Jain, “Learning face age progression: A pyramid architecture of gans”, in *2018 IEEE/CVF Conference on Computer Vision and Pattern Recognition*, pp.31–39, 2018.
- [12] K. Olszewski, D. Ceylan, J. Xing, J. Echevarria, *et al.*, “Intuitive, interactive beard and hair synthesis with generative models”, in *2020 IEEE/CVF Conference on Computer Vision and Pattern Recognition (CVPR)*, pp.7444–7454, 2020.
- [13] W. Wang, X. Alameda-Pineda, D. Xu, P. Fua, *et al.*, “Every smile is unique: Landmark-guided diverse smile generation”, in *2018 IEEE/CVF Conference on Computer Vision and Pattern Recognition*, pp.7083–7092, 2018.
- [14] Y. Shen, J. Gu, X. Tang, and B. Zhou, “Interpreting the latent space of gans for semantic face editing”, in *2020 IEEE/CVF Conference on Computer Vision and Pattern Recognition (CVPR)*, pp.9240–9249, 2020.
- [15] P. Zhuang, O. Koyejo, and A. G. Schwing, “Enjoy your editing: Controllable gans for image editing via latent space navigation”, in *9th International Conference on Learning Representations, ICLR 2021*, pp.1–16, 2021.
- [16] Y. Jiang, Z. Huang, T. Wu, X. Pan, *et al.*, “Talk-to-edit: Fine-grained 2d and 3d facial editing via dialog”, *IEEE Transactions on Pattern Analysis and Machine Intelligence*, vol.46, no.5, pp.3692–3706, 2024.
- [17] M. Wang, X.-Q. Lyu, Y.-J. Li, and F.-L. Zhang, “Vr content creation and exploration with deep learning: A survey”, *Computational Visual Media*, vol.6, pp.3–28, 2020.
- [18] F. Arena, M. Collotta, G. Pau, and F. Termine, “An overview of augmented reality”, *Computers*, vol.11, no.2, article no.28, 2022.
- [19] S. Ryu, K. Ko, and J. W.-K. Hong, “Performance analysis of applying deep learning for virtual background of webrtc-based video conferencing system”, in *2021 22nd Asia-Pacific Network Operations and Management Symposium (APNOMS)*, pp.53–56, 2021.
- [20] T. Karras, S. Laine, and T. Aila, “A style-based generator architecture for generative adversarial networks”, in *2019 IEEE/CVF Conference on Computer Vision and Pattern Recognition (CVPR)*, pp.4396–4405, 2019.
- [21] B. Kawar, S. Zada, O. Lang, O. Tov, *et al.*, “Imagic: Text-based real image editing with diffusion models”, in *2023 IEEE/CVF Conference on Computer Vision and Pattern Recognition (CVPR)*, pp.6007–6017, 2023.
- [22] T. Wu, Z. Chen, D. He, L. Qian, *et al.*, “Cddm: Channel denoising diffusion models for wireless semantic communications”, *IEEE Transactions on Wireless Communications*, vol.23, no.9, pp.11168–11183, 2024.
- [23] W. Xie, M. Xiong, Z. Ren, J. Wang, and Z. Yang, “Research on semantic communication based on joint control mechanism of shallow and deep neural network”, *Chinese Journal of Electronics*, vol.34, no.2, pp.698–711, 2025.
- [24] X. Han, Y. Wu, Z. Gao, B. Feng, *et al.*, “Scsc: A novel standards-compatible semantic communication framework for image transmission”, *IEEE Transactions on Communications*, vol.73, no.8, pp.5682–5698, 2025.
- [25] H. Li, H. Tong, S. Wang, N. Yang, *et al.*, “Video semantic communication with major object extraction and contextual video encoding”, in *2024 IEEE Wireless Communications and Networking Conference (WCNC)*, pp.1–6, 2024.
- [26] D. A. Hudson and C. D. Manning, “Compositional attention networks for machine reasoning”, in *International Conference on Learning Representations*, 2018.
- [27] F. Jiang, C. Tang, L. Dong, K. Wang, *et al.*, “Visual language model-based cross-modal semantic communication systems”, *IEEE Transactions on Wireless Communications*, vol.24, no.5, pp.3937–3948, 2025.
- [28] Y. Tian, J. Ying, Z. Qin, Y. Jin, and X. Tao, “Synchronous multi-modal semantic communication system with packet-level coding”, *IEEE Transactions on Wireless Communications*, vol.24, no.5, pp.3684–3697, 2025.
- [29] E. Erdemir, T.-Y. Tung, P. L. Dragotti, and D. Gündüz, “Generative joint source-channel coding for semantic image transmission”, *IEEE Journal on Selected Areas in Communications*, vol.41, no.8, pp.2645–2657, 2023.
- [30] S. F. Yilmaz, C. Karamanlı, and D. Gündüz, “Distributed deep joint source-channel coding over a multiple access channel”, in *ICC 2023 - IEEE International Conference on Communications*, pp.1400–1405, 2023.
- [31] T.-Y. Tung and D. Gündüz, “Deep joint source-channel and encryption coding: Secure semantic communications”, in *ICC 2023 - IEEE International Conference on Communications*, pp.5620–5625, 2023.
- [32] N. Tishby and N. Zaslavsky, “Deep learning and the information bottleneck principle”, in *2015 IEEE Information Theory Workshop (ITW)*, pp.1–5, 2015.
- [33] A. M. Saxe, Y. Bansal, J. Dapello, M. Advani, *et al.*, “On the information bottleneck theory of deep learning”, in *International Conference on Learning Representations*, 2018.
- [34] J. Shao, Y. Mao, and J. Zhang, “Learning task-oriented communication for edge inference: An information bottleneck approach”, *IEEE Journal on Selected Areas in Communications*, vol.40, no.1, pp.197–211, 2022.

- [35] T. M. Cover, *Elements of information theory*, John Wiley & Sons, New York, USA, chapter 2.8, pp.34–35, 1999.
- [36] I. Goodfellow, J. Pouget-Abadie, M. Mirza, B. Xu, *et al.*, “Generative adversarial networks”, *Communications of the ACM*, vol.63, no.11, pp.139–144, 2020.
- [37] W. Xia, Y. Zhang, Y. Yang, J.-H. Xue, *et al.*, “Gan inversion: A survey”, *IEEE Transactions on Pattern Analysis and Machine Intelligence*, vol.45, no.3, pp.3121–3138, 2023.
- [38] W. Yu, H. Fang, B. Chen, X. Sui, *et al.*, “Gi-nas: Boosting gradient inversion attacks through adaptive neural architecture search”, *IEEE Transactions on Information Forensics and Security*, vol.20, pp.7648–7662, 2025.
- [39] H. Fang, Y. Qiu, H. Yu, W. Yu, *et al.*, “Privacy leakage on dnns: A survey of model inversion attacks and defenses”, *arXiv preprint arXiv:2402.04013*, in press, 2024.
- [40] H. Fang, J. Kong, W. Yu, B. Chen, *et al.*, “One perturbation is enough: On generating universal adversarial perturbations against vision-language pre-training models”, in *Proceedings of the IEEE/CVF International Conference on Computer Vision*, pp.4090–4100, 2025.
- [41] Y. Qiu, H. Yu, H. Fang, W. Yu, *et al.*, “Mibench: A comprehensive benchmark for model inversion attack and defense”, in press, 2024.
- [42] Y. Qiu, H. Yu, H. Fang, T. Zhuang, *et al.*, “Mibench: A comprehensive framework for benchmarking model inversion attack and defense”, *arXiv preprint arXiv:2410.05159*, in press, 2024.
- [43] R. Zhang, P. Isola, A. A. Efros, E. Shechtman, and O. Wang, “The unreasonable effectiveness of deep features as a perceptual metric”, in *2018 IEEE/CVF Conference on Computer Vision and Pattern Recognition*, pp.586–595, 2018.
- [44] Y. Jiang, Z. Huang, X. Pan, C. C. Loy, and Z. Liu, “Talk-to-edit: Fine-grained facial editing via dialog”, in *2021 IEEE/CVF International Conference on Computer Vision (ICCV)*, pp.13779–13788, 2021.
- [45] S. Hochreiter and J. Schmidhuber, “Long short-term memory”, *Neural Computation*, vol.9, no.8, pp.1735–1780, 1997.
- [46] E. Boursoulatzé, D. Burth Kurka, and D. Gündüz, “Deep joint source-channel coding for wireless image transmission”, *IEEE Transactions on Cognitive Communications and Networking*, vol.5, no.3, pp.567–579, 2019.
- [47] J. Deng, J. Guo, N. Xue, and S. Zafeiriou, “Arcface: Additive angular margin loss for deep face recognition”, in *2019 IEEE/CVF Conference on Computer Vision and Pattern Recognition (CVPR)*, pp.4685–4694, 2019.
- [48] Z. Chen, Y. Duan, W. Wang, J. He, *et al.*, “Vision transformer adapter for dense predictions”, in *The Eleventh International Conference on Learning Representations*, 2023.
- [49] H. Chen, R. Tao, H. Zhang, Y. Wang, *et al.*, “Conv-adapter: Exploring parameter efficient transfer learning for convnets”, in *2024 IEEE/CVF Conference on Computer Vision and Pattern Recognition Workshops (CVPRW)*, pp.1551–1561, 2024.
- [50] Z. Liu, P. Luo, X. Wang, and X. Tang, “Deep learning face attributes in the wild”, in *2015 IEEE International Conference on Computer Vision (ICCV)*, pp.3730–3738, 2015.
- [51] T. Karras, T. Aila, S. Laine, and J. Lehtinen, “Progressive growing of gans for improved quality, stability, and variation”, in *International Conference on Learning Representations*, 2018.
- [52] T. Karras, M. Aittala, J. Hellsten, S. Laine, *et al.*, “Training generative adversarial networks with limited data”, *Advances in neural information processing systems*, vol.33, pp.12104–12114, 2020.
- [53] G. Wallace, “The jpeg still picture compression standard”, *IEEE Transactions on Consumer Electronics*, vol.38, no.1, pp.xviii–xxxiv, 1992.
- [54] R. Gallager, “Low-density parity-check codes”, *IRE Transactions on Information Theory*, vol.8, no.1, pp.21–28, 1962.
- [55] M. Heusel, H. Ramsauer, T. Unterthiner, B. Nessler, and S. Hochreiter, “Gans trained by a two time-scale update rule converge to a local nash equilibrium”, *Advances in neural information processing systems*, vol.30, 2017.
- [56] M. Bińkowski, D. J. Sutherland, M. Arbel, and A. Gretton, “Demystifying mmd gans”, in *International Conference on Learning Representations*, 2018.
- [57] A. Radford, J. W. Kim, C. Hallacy, A. Ramesh, *et al.*, “Learning transferable visual models from natural language supervision”, in *Proceedings of the 38th International Conference on Machine Learning*, PMLR, *Proceedings of Machine Learning Research*, vol.139, pp.8748–8763, 2021.
- [58] M. I. Belghazi, A. Baratin, S. Rajeshwar, S. Ozair, *et al.*, “Mutual information neural estimation”, in *Proceedings of the 35th International Conference on Machine Learning*, PMLR, *Proceedings of Machine Learning Research*, vol.80, pp.531–540, 2018.
- [59] J. Gou, B. Yu, S. J. Maybank, and D. Tao, “Knowledge distillation: A survey”, *International journal of computer vision*, vol.129, no.6, pp.1789–1819, 2021.
- [60] Y. Wang, C. Yang, S. Lan, L. Zhu, and Y. Zhang, “End-edge-cloud collaborative computing for deep learning: A comprehensive survey”, *IEEE Communications Surveys & Tutorials*, vol.26, no.4, pp.2647–2683, 2024.